Anal. Chem. **2010,** *82,* 7979–7986

Molecular Characterization of Organic Aerosols Using Nanospray-Desorption/Electrospray Ionization-Mass Spectrometry†

Patrick J. Roach,‡ Julia Laskin,*,‡ and Alexander Laskin*,§

Chemical and Materials Sciences Division and William R. Wiley Environmental and Molecular Sciences Laboratory, Pacific Northwest National Laboratory, P.O. Box 999, MSIN K8-88, Richland, Washington 99352

Nanospray desorption electrospray ionization (nano-DESI) combined with high-resolution mass spectrometry (HR-MS) is a promising approach for the detailed, molecular-level chemical characterization of atmospheric organic aerosols (OA) collected in laboratory and field experiments. The nano-DESI technique possesses distinct advantages of technical simplicity, enhanced sensitivity, and signal stability. In nano-DESI, analyte is desorbed into a solvent bridge formed between two capillaries and the analysis surface, which enables fast and efficient characterization of OA collected on substrates without sample preparation. Stable signals achieved using nano-DESI make it possible to obtain high-quality HR-MS data both for laboratory-generated and field-collected OA using only a small amount of material (<10 ng). Furthermore, nano-DESI enables the efficient detection of chemically labile compounds in OA, which is important for understanding chemical aging phenomena.

Atmospheric aerosols interact with incoming solar radiation and modify cloud properties resulting in significant impacts on climate, air quality, and human health.[1−6] An area of vast uncertainty is the composition and atmospheric chemistry of organic aerosols (OA), which are either emitted as primary OA from a variety of sources including industrial processes, combustion of fossil fuels, and biomass burning or formed as a result of gas-to-particle partitioning in atmospheric physicochemical processes that form secondary OA. The most important climate-related physical properties of OA, such as their ability to absorb or reflect solar radiation and hygroscopicity, are determined by molecular composition.

Characterizing the molecular composition and chemical transformations of OA is a major challenges in atmospheric aerosol research. Recent field studies[7−16] have demonstrated that about 50−80% of OA is composed of high molecular weight (M_w) compounds that cannot be characterized with sufficient detail using traditional analytical approaches. High-resolution mass spectrometry (HR-MS) coupled with soft ionization methods such as electrospray ionization (ESI)[17] is the technique of choice for the structural characterization of individual molecules in complex mixtures of OA. The utility of high-resolution ESI-MS for the analysis of environmental samples has been demonstrated in a number of recent studies[18−38] focused on the chemical characterization of laboratory generated aerosols, water-soluble organics, ambient aerosols, and cloud/fogwater

† Part of the special issue "Atmospheric Analysis as Related to Climate Change".

* To whom correspondence should be addressed. E-mail: Julia.Laskin@pnl.gov (J.L.); Alexander.Laskin@pnl.gov (A.L.).

‡ Chemical and Materials Sciences Division.

§ William R. Wiley Environmental and Molecular Sciences Laboratory.

(1) Seinfeld, J. H.; Pankow, J. F. *Annu. Rev. Phys. Chem.* **2003**, *54*, 121–140.
(2) Poschl, U. *Angew. Chem., Int. Ed.* **2005**, *44*, 7520–7540.
(3) Simoneit, B. R. T. *Appl. Geochem.* **2002**, *17*, 129–162.
(4) Andreae, M. O.; Gelencser, A. *Atmos. Chem. Phys.* **2006**, *6*, 3131–3148.
(5) Rosenfeld, D.; Lohmann, U.; Raga, G. B.; O'Dowd, C. D.; Kulmala, M.; Fuzzi, S.; Reissell, A.; Andreae, M. O. *Science* **2008**, *321*, 1309–1313.
(6) Unger, N.; Shindell, D. T.; Koch, D. M.; Streets, D. G. *J. Geophys. Res.* **2008**, *113*, D02306, DOI: 10.1029/2007JD008683.
(7) Mayol-Bracero, O. L.; Guyon, P.; Graham, B.; Roberts, G.; Andreae, M. O.; Decesari, S.; Facchini, M. C.; Fuzzi, S.; Artaxo, P. *J. Geophys. Res.-Atmos.* **2002**, 107.
(8) Samburova, V.; Zenobi, R.; Kalberer, M. *Atmos. Chem. Phys.* **2005**, *5*, 2163–2170.
(9) Baltensperger, U.; Kalberer, M.; Dommen, J.; Paulsen, D.; Alfarra, M. R.; Coe, H.; Fisseha, R.; Gascho, A.; Gysel, M.; Nyeki, S.; Sax, M.; Steinbacher, M.; Prevot, A. S. H.; Sjogren, S.; Weingartner, E.; Zenobi, R. *Faraday Discuss.* **2005**, *130*, 265–278.
(10) Yang, H.; Xu, J. H.; Wu, W. S.; Wan, C. H.; Yu, J. Z. *Environ. Chem.* **2004**, *1*, 13–17.
(11) Falkovich, A. H.; Graber, E. R.; Schkolnik, G.; Rudich, Y.; Maenhaut, W.; Artaxo, P. *Atmos. Chem. Phys.* **2005**, *5*, 781–797.
(12) Hoffer, A.; Gelencser, A.; Blazso, M.; Guyon, P.; Artaxo, P.; Andreae, M. O. *Atmos. Chem. Phys.* **2006**, *6*, 3505–3515.
(13) Kalberer, M.; Sax, M.; Samburova, V. *Environ. Sci. Technol.* **2006**, *40*, 5917–5922.
(14) Gross, D. S.; Galli, M. E.; Kalberer, M.; Prevot, A. S. H.; Dommen, J.; Alfarra, M. R.; Duplissy, J.; Gaeggeler, K.; Gascho, A.; Metzger, A.; Baltensperger, U. *Anal. Chem.* **2006**, *78*, 2130–2137.
(15) Denkenberger, K. A.; Moffet, R. C.; Holecek, J. C.; Rebotier, T. P.; Prather, K. A. *Environ. Sci. Technol.* **2007**, *41*, 5439–5446.
(16) Wang, X.; Gao, S.; Yang, X.; Chen, H.; Chen, J.; Zhuang, G.; Surratt, J. D.; Chan, M.-N.; Seinfeld, J. H. *Environ. Sci. Technol.* **2010**, *44*, 4441–4446.
(17) Fenn, J. B.; Mann, M.; Meng, C. K.; Wong, S. F.; Whitehouse, C. M. *Science* **1989**, *246*, 64–71.
(18) Fievre, A.; Solouki, T.; Marshall, A. G.; Cooper, W. T. *Energy Fuels* **1997**, *11*, 554–560.
(19) Kujawinski, E. B.; Hatcher, P. G.; Freitas, M. A. *Anal. Chem.* **2002**, *74*, 413–419.
(20) Tolocka, M. P.; Jang, M.; Ginter, J. M.; Cox, F. J.; Kamens, R. M.; Johnston, M. V. *Environ. Sci. Technol.* **2004**, *38*, 1428–1434.
(21) Stenson, A. C.; Landing, W. M.; Marshall, A. G.; Cooper, W. T. *Anal. Chem.* **2002**, *74*, 4397–4409.
(22) Kalberer, M.; Paulsen, D.; Sax, M.; Steinbacher, M.; Dommen, J.; Prevot, A. S. H.; Fisseha, R.; Weingartner, E.; Frankevich, V.; Zenobi, R.; Baltensperger, U. *Science* **2004**, *303*, 1659–1662.
(23) Reemtsma, T.; These, A.; Springer, A.; Linscheid, M. *Environ. Sci. Technol.* **2006**, *40*, 5839–5845.

10.1021/ac101449p
Published on Web 07/28/2010

samples. In these studies, OA samples were either collected or prepared as extracts in organic or mixed organic/water solutions. More recent studies have employed the novel desorption electrospray ionization (DESI)[39−41] technique for the analysis of OA samples collected on substrates in field and laboratory studies.[42−44] DESI is an ambient ionization technique[44−47] which enables the rapid and sensitive characterization of analytes on surfaces in their native environment without sample preparation, and therefore is ideally suited for the direct analysis of OA samples deposited on substrates. In addition, DESI has an important advantage of a short solvent residence time for OA constituents, which minimizes solution-phase dissociation of labile organic compounds present in OA and provides information on the composition of aerosol samples that cannot be obtained using ESI-MS.[44]

Despite these advantages, DESI characterization of OA is often challenging because it is difficult to maintain a stable MS signal over a significant period of time. Recently we developed a novel approach termed nanospray desorption electrospray ionization (nano-DESI)[48] that overcomes some of the limitations of DESI and enables exquisite control of the ion formation and transfer processes by separating desorption and ionization steps. Nano-DESI allows efficient desorption and sensitive analysis of extremely small quantities of substrate deposited organic materials. In this approach the analyte deposited on a substrate is probed in an ambient environment by a liquid bridge of charged solvent formed at the junction between two capillaries as shown in Figure 1. One primary capillary is used to create and maintain a charged droplet of solvent on the substrate while a second capillary creates a self-aspirating nanospray of solvent containing dissolved analyte that is directed into the inlet of a mass spectrometer. Nano-DESI enables the efficient collection, ionization, and transfer of analyte resulting in a significant improvement of detection limits while retaining the most important tenets of DESI-MS: simplicity, no requirement for special sample preparation or pretreatment, and speed of analysis. Here we demonstrate for the first time the utility of nano-DESI for characterizing the molecular composition of both laboratory generated and field collected OA samples. We show that nano-DESI combined with high-resolution mass spectrometry (HR-MS) can be used for the detailed analysis of relatively small amounts (<10 ng) of OA collected on substrates.

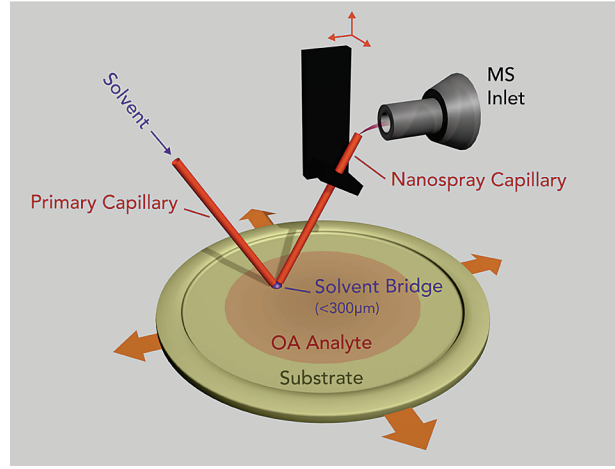

Figure 1. Schematic of nano-DESI source configuration for analysis of OA samples.

EXPERIMENTAL SECTION

Preparation and Collection of OA Samples. A 10 stage rotating micro-orifice uniform deposit impactor (MOUDI) model 110R (MSP, Inc.) was used to deposit OA particles on substrates for nano-DESI/HR-MS analysis. MOUDI employs a large number of micro-orifice nozzles and rotating impaction plates so that the collected particles are spread out uniformly over a 27 mm diameter impaction area on a 47 mm substrate. The OA samples described in this manuscript were collected on the eighth stage of MOUDI, which corresponds to particles in a size range of 0.18−0.32 μm aerodynamic diameter. The eighth stage was chosen to facilitate comparison with our previous reports on ESI-MS and DES-MS analysis of OA samples.[27,31,32,34,44] Figure S1 in the Supporting Information shows a photo of a typical sample collected on the eighth stage of MOUDI. The model 110R has a sampling rate of 30 slpm (standard liters per minute).

Limonene secondary OA samples were created, as in previous investigations,[26,29,34,44] by the ozone-initiated oxidation of D-limonene vapor in an inflatable Teflon reaction chamber and

(24) Surratt, J. D.; Murphy, S. M.; Kroll, J. H.; Ng, N. L.; Hildebrandt, L.; Sorooshian, A.; Szmigielski, R.; Vermeylen, R.; Maenhaut, W.; Claeys, M.; Flagan, R. C.; Seinfeld, J. H. *J. Phys. Chem. A* **2006**, *110*, 9665–9690.
(25) Reinhardt, A.; Emmenegger, C.; Gerrits, B.; Panse, C.; Dommen, J.; Baltensperger, U.; Zenobi, R.; Kalberer, M. *Anal. Chem.* **2007**, *79*, 4074–4082.
(26) Heaton, K. J.; Dreyfus, M. A.; Wang, S.; Johnston, M. V. *Environ. Sci. Technol.* **2007**, *41*, 6129–6136.
(27) Walser, M. L.; Desyaterik, Y.; Laskin, J.; Laskin, A.; Nizkorodov, S. A. *Phys. Chem. Chem. Phys.* **2008**, *10*, 1009–1022.
(28) Altieri, K. E.; Seitzinger, S. P.; Carlton, A. G.; Turpin, B. J.; Klein, G. C.; Marshall, A. G. *Atmos. Environ.* **2008**, *42*, 1476–1490.
(29) Bateman, A. P.; Walser, M. L.; Desyaterik, Y.; Laskin, J.; Laskin, A.; Nizkorodov, S. A. *Environ. Sci. Technol.* **2008**, *42*, 7341–7346.
(30) Wozniak, A. S.; Bauer, J. E.; Sleighter, R. L.; Dickhut, R. M.; Hatcher, P. G. *Atmos. Chem. Phys.* **2008**, *8*, 5099–5111.
(31) Smith, J. S.; Laskin, A.; Laskin, J. *Anal. Chem.* **2009**, *81*, 1512–1521.
(32) Laskin, A.; Smith, J. S.; Laskin, J. *Environ. Sci. Technol.* **2009**, *43*, 3764–3771.
(33) Heaton, K. J.; Sleighter, R. L.; Hatcher, P. G.; Hall, W. A., IV; Johnston, M. V. *Environ. Sci. Technol.* **2009**, *43*, 7797–7802.
(34) Bateman, A. P.; Nizkorodov, S. A.; Laskin, J.; Laskin, A. *Phys. Chem. Chem. Phys.* **2009**, *11*, 7931–7942.
(35) Nguyen, T. B.; Bateman, A. P.; Bones, D. L.; Nizkorodov, S. A.; Laskin, J.; Laskin, A. *Atmos. Environ.* **2010**, *44*, 1032–1042.
(36) Reemtsma, T.; These, A.; Venkatachari, P.; Xia, X. Y.; Hopke, P. K.; Springer, A.; Linscheid, M. *Anal. Chem.* **2006**, *78*, 8299–8304.
(37) Mazzoleni, L. R.; Ehrmann, B. M.; Shen, X.; Marshall, A. G.; Collett, J. L. *Environ. Sci. Technol.* **2010**, *44*, 3690–3697.
(38) Altieri, K. E.; Turpin, B. J.; Seitzinger, S. P. *Atmos. Chem. Phys.* **2009**, *9*, 2533–2542.
(39) Takats, Z.; Wiseman, J. M.; Gologan, B.; Cooks, R. G. *Science* **2004**, *306*, 471–473.
(40) Takats, Z.; Wiseman, J. M.; Cooks, R. G. *J. Mass Spectrom.* **2005**, *40*, 1261–1275.
(41) Cooks, R. G.; Ouyang, Z.; Takats, Z.; Wiseman, J. M. *Science* **2006**, *311*, 1566–1570.
(42) Li, M.; Chen, H.; Yang, X.; Chen, J. M.; Li, C. L. *Atmos. Environ.* **2009**, *43*, 2717–2720.
(43) Li, M.; Chen, H.; Wang, B. F.; Yang, X.; Lian, J. J.; Chen, J. M. *Int. J. Mass Spectrom.* **2009**, *281*, 31–36.
(44) Laskin, J.; Laskin, A.; Roach, P. J.; Slysz, G. W.; Anderson, G. A.; Nizkorodov, S. A.; Bones, D. L.; Nguyen, L. Q. *Anal. Chem.* **2010**, *82*, 2048–2058.
(45) Harris, G. A.; Nyadong, L.; Fernandez, F. M. *Analyst* **2008**, *133*, 1297–1301.
(46) Van Berkel, G. J.; Pasilis, S. P.; Ovchinnikova, O. *J. Mass Spectrom.* **2008**, *43*, 1161–1180.
(47) Chen, H.; Gamez, G.; Zenobi, R. *J. Am. Soc. Mass. Spectrom.* **2009**, *20*, 1947–1963.
(48) Roach, P. J.; Laskin, J.; Laskin, A. *Analyst* **2010**, DOI: 10.1039/C0AN00312C.

collected onto Teflon (polytetrafluoroethylene, PTFE) 46.2 mm ring supported membranes (Whatman, Inc.). Freshly prepared (white) limonene secondary OA samples were first analyzed using the nano-DESI approach, then the remaining sample was extracted using the same solvents for ESI-MS analysis. The limonene secondary OA sample was also chemically aged in the presence of gas-phase ammonia, which results in the formation of N-containing species responsible for "browning" of the aged (brown) limonene secondary OA.[44,49] For aging experiments, the sample was placed onto a plastic plate and exposed to a gas-phase mixture of NH_3, HNO_3, and H_2O by floating the plate in a covered Petri dish containing 0.1 M aqueous solution of NH_4NO_3 (Aldrich Inc., 99.99% purity). In this experiment the limonene secondary OA sample was exposed to an equilibrium partial pressures of $NH_3(g)$ ($<1.2 \times 10^{-7}$ atm), and $HNO_3(g)$ ($<1.6 \times 10^{-13}$ atm) for 24 h. Additional details of these experiments are published elsewhere.[44]

Biomass burning OA samples were collected during the FLAME 2006 experiment conducted at the U.S. Forest Service Fire Science Laboratory (FSL, Missoula, MT) where a series of laboratory measurements and the aerosol sampling of biomass burning emissions were performed (http://chem.atmos.colostate.edu/FLAME/). Our previous studies[31,32] showed that burns of biomass composed of dried ponderosa pine needles and sticks (PPNS) produced smoke especially rich in OA material, which has a large number of distinct chemical signature compounds characterized by our previous ESI/HR-MS analysis. Specifically, a large number of highly oxidized polar species[31] and N-containing heterocyclic compounds[32] with a relatively high M_w (<700 m/z) were identified and reported for that sample. In these nano-DESI experiments, a piece of the same biomass burning OA sample that has been left aside during solvent extraction ESI studies was later reanalyzed using the nano-DESI approach. The biomass burning OA sample was collected on an aluminum foil substrate.

Mexico City OA samples were collected during the MILAGRO 2006 field experiment at the T0 sampling site.[50] The T0 sampling site was located in the northern part of Mexico City, on the campus of "Instituto Mexicano del Petroleo" at the rooftop of a five story research building, ~20 m above the ground. The two samples collected on the eighth stage of the MOUDI during two 3 h time periods from the early morning (6 a.m.−9 a.m.) and around noon (11 a.m.−2 p.m.) on March 27, 2006 were selected for nano-DESI/HR-MS analysis. The selection of these two samples was motivated by characteristic diurnal changes in OA chemistry that has been associated with photochemical oxidation processes that are reported in numerous publications from MILAGRO and previous studies conducted in Mexico City (see ref 51 and references therein). Both samples were collected onto Teflon substrates.

Mass Spectrometry. Samples were analyzed using a LTQ-Orbitrap HR-MS (Thermo Electron, Bremen, Germany) equipped with a commercial DESI source (Prosolia, Inc., Indianapolis, IN) that was modified to accommodate nano-DESI and ESI sources. For ESI experiments, solvent extracts were prepared by the ultrasonic washing of substrates in 1 mL of acetonitrile. Sample extracts were injected through a pulled, fused silica capillary (50 μm i.d.) at a flow rate of 0.3−1.0 μL/min using a spray voltage of 3.5−4.2 kV. Nano-DESI analysis was performed for samples collected on Teflon or aluminum foil substrates using silica capillaries (193 μm o.d.) at the following conditions: spray voltage of 3−5 kV, 0.5 mm distance from the tip of the nanospray capilary to the heated inlet of the LTQ-Orbitrap, 0.3−0.9 μL/min flow rate.[48] The substrate deposited OA samples were first attached to a glass microscope slide using cellophane tape and then mounted on the Prosolia ion source stage without additional preparation. Nano-DESI solvents were 1:1 (volume) mixtures of acetonitrile (AcN) and water and methanol (MeOH) and water. The mass spectrometer was operated in the positive-ion mode with a resolving power of 60 000 at m/z 400. The instrument was calibrated using a standard mixture of caffeine, MRFA, and Ultramark 1621 (calibration mix MSCAL 5, Sigma-Aldrich, Inc.).

Figure 1 shows a schematic of the nano-DESI source[48] configuration. The primary capillary is used to supply solvent to the nanospray capillary forming a solvent bridge between the two. A several kiloelectronvolt potential is created between an electrode placed in line with the solvent supply capillary and the MS inlet. The solvent is conductive, thus the potential is transferred through the continuous liquid circuit to the emitting end of the nanospray capillary. The high field gradient created between the capillary tip and the grounded MS inlet results in nanospray emission. Liquid removed from the circuit by the nanospray process is replenished continuously with a syringe pump to maintain the volume of the bridge. The bridge is brought into contact with an analyte-containing substrate allowing the analyte to be dissolved from the substrate and transported with the solvent into the heated capillary of the LTQ-Orbitrap MS.

The analyte is sampled from the area that is contacted by the liquid bridge. The size of this sampling area is determined by the volume of the liquid bridge, which is controlled by varying the speed of the syringe pump with respect to the self-aspiration rate of nanospray. The self-aspiration rate can be controlled by either reducing/pulling the nanospray capillary emitter tip to a smaller diameter or reducing the potential gradient at the spray tip to reduce the aspiration rate or doing the converse to increase it. In general, lower aspiration rates (<600 nL/min) are desirable to maintain a stable bridge volume with minimal effort.

Data Analysis and Processing. A nano-DESI analysis routine was developed for background subtraction to distinguish the mass peaks that were attributable to the sample from those that were attributable to background peaks that originated from the substrate or the solvent. The OA samples collected by MOUDI exhibit two distinguishable domains on the impaction substrate. The first domain is the center where deposited aerosol was present, and the second domain is the edge where OA analyte was not present (see Figure S1 in the Supporting Information for illustration). Time-dependent MS signal was acquired using the "LC acquire" capability of the Xcalibur software (Thermo Electron, Inc.). The

(49) Bones, D. L.; Henricksen, D. K.; Mang, S. A.; Gonsior, M.; Bateman, A. P.; Nguyen, T. B.; Cooper, W. J.; Nizkorodov, S. A. *J. Geophys. Res.-Atmos.* **2010**, 115.

(50) Moffet, R. C.; Henn, T. R.; Tivanski, A. V.; Hopkins, R. J.; Desyaterik, Y.; Kilcoyne, A. L. D.; Tyliszczak, T.; Fast, J.; Barnard, J.; Shutthanandan, V.; Cliff, S. S.; Perry, K. D.; Laskin, A.; Gilles, M. K. *Atmos. Chem. Phys.* **2010**, *10*, 961–976.

(51) Molina, L. T.; Madronich, S.; Gaffney, J. S.; Apel, E.; de Foy, B.; Fast, J.; Ferrare, R.; Herndon, S.; Jimenez, J. L.; Lamb, B.; Osornio-Vargas, A. R.; Russell, P.; Schauer, J. J.; Stevens, P. S.; Zavala, M. *Atmos. Chem. Phys. Discuss.* **2010**, *10*, 7819–7983.

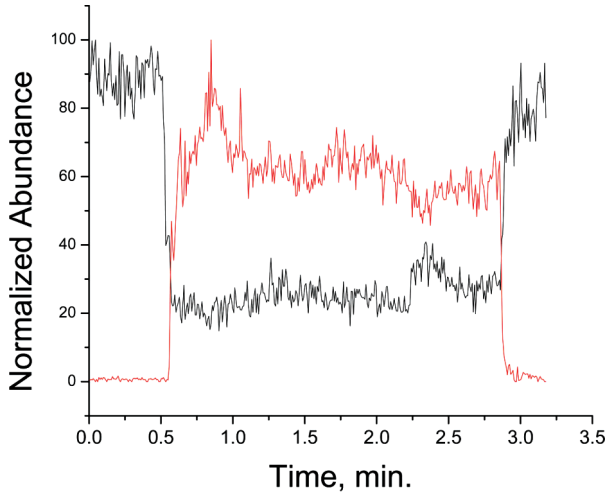

Figure 2. Typical time dependent signal intensity of mass peaks representing an analyte peak (red) and a background peak (black).

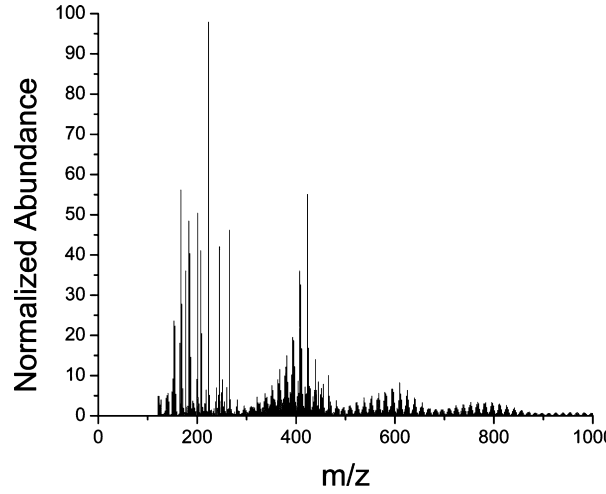

Figure 3. Nano-DESI mass spectrum of fresh (white) limonene secondary OA sample.

first 0.5 min of the LC acquisition was obtained with the nano-DESI liquid bridge in contact with the edge domain, which did not contain OA. Then, the substrate was translated such that the probe was located within the center, OA containing area, and the probe was left stationary for 2.5 min. Finally the stage was returned to the edge domain and again left stationary for 0.5 min. Two exemplary abundance traces, which represent the time-dependent characteristics of the OA analyte (red) and the background signal (black) are shown in Figure 2.

The time-dependent mass spectra were then analyzed using a suite of programs developed at PNNL. Decon2LS[52] (http://ncrr.pnl.gov/software/) was employed to reduce the many individual scans from the .raw file of the LC acquisition into approximately a dozen boxcar averaged spectra representative of the time domain signal and then extract the mass spectral features with a signal-to-noise ratio of 3 or higher. The LC analysis program VIPER[53] (http://ncrr.pnl.gov/software/) was then used to cluster the identified peaks between the averaged spectra. Clustering of mass spectra aligns the signal intensities observed in experimental spectra along a common m/z axis to facilitate peak identification and comparison of spectral data obtained for different samples or settings. Clustering was performed using a mass tolerance of 5 ppm. The clustered peaks were subsequently analyzed using a collection of custom macros created with Excel VBA to characterize the time-dependent abundance of each peak. The background peaks were identified and separated from the analyte peaks based on an analysis of the time-dependent signal intensity shown in Figure 2. Analyte-related peaks were then assigned molecular formula using the freeware program, Formula Calculator v. 1.1 (http://magnet.fsu.edu/~midas/download.html).

RESULTS AND DISCUSSION

A nano-DESI mass spectrum obtained from the analysis of fresh (white) limonene secondary OA using the 1:1 (v/v) AcN/water spray solvent is shown in Figure 3. The mass spectrum possesses five distinct peak manifolds that are centered on 200, 400, 600, 800, and 1000 m/z that can be attributed to oligomer products representing the monomeric through the pentameric species, respectively. Our previous investigations involving the ESI and DESI sources have produced similar results.[26,34,44] In this study, a liquid bridge volume of ~0.5 μL maintained on the sample produced a stable and intense signal for longer than 10 min. The stability of the signal is determined by the exquisite control of desorption, ionization, and transport of the analyte in nano-DESI experiments, which slows down analyte consumption extending the length of usable signal and hence significantly reduces the amount of sample required for analysis. The amount of limonene secondary OA material probed in the nano-DESI experiment can be easily estimated. The total mass (80 ± 10 μg) of the limonene secondary OA that is deposited onto the eighth stage of the MOUDI impactor is distributed over a circular spot that is 27 mm in diameter (Figure S1 in the Supporting Information). Assuming uniform deposition of limonene secondary OA over the OA containing area and a nano-DESI solvent bridge contact area of 300 μm in diameter,[48] we estimate that the sampled area contains approximately 10 ng of limonene secondary OA, while only a small part of it is consumed during the analysis.

Our previous study[44] demonstrated a number of the unique advantages of DESI analysis of OA for the detailed characterization of chemically labile constituents that could not be detected using ESI-MS. Chemical aging of the limonene secondary OA results in the formation of N-containing molecules that absorb visible light and result in browning of the sample. The formation of N-containing molecules has been attributed to the reactions of aldehydes or ketones with ammonia that result in formation of imines and oligomeric products containing —C—N=C— bonds linking together monomeric molecules of fresh (white) limonene secondary OA.[44] This reaction mechanism is acid-catalyzed and reversible; the resulting products are therefore unstable in the acidified solvents.[44,49] Indeed, our previous study showed that a significant number of N-containing compounds produced by the chemical aging of limonene secondary OA in the presence of gaseous ammonia undergo acid-catalyzed hydrolysis in solvent extracts and, consequently, cannot be detected using ESI-MS. In contrast, these chemically labile compounds are readily observed using DESI-MS experiments.

(52) Jaitly, N.; Mayampurath, A.; Littlefield, K.; Adkins, J. N.; Anderson, G. A.; Smith, R. D. *BMC Bioinf.* **2009**, *10*, 87.
(53) Monroe, M. E.; Tolic, N.; Jaitly, N.; Shaw, J. L.; Adkins, J. N.; Smith, R. D. *Bioinformatics* **2007**, *23*, 2021–2023.

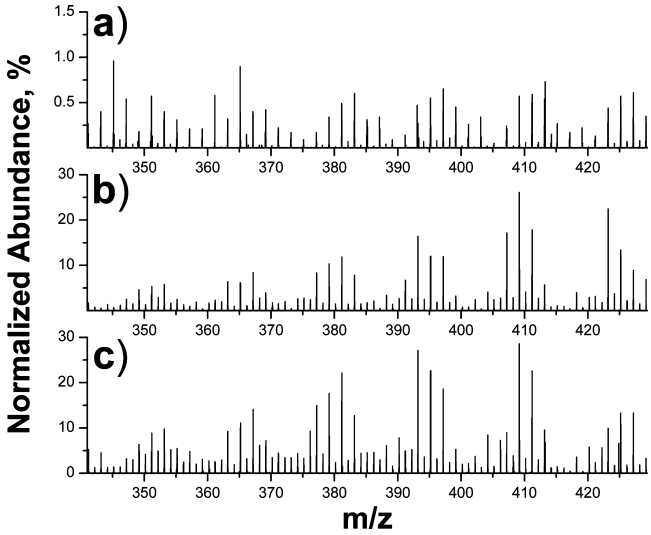

Figure 4. Comparison of aged (brown) limonene secondary OA mass spectra obtained by (a) ESI, (b) DESI, and (c) nano-DESI. The signal was normalized to the largest peak in the spectrum acquired over a broad mass range of m/z 120−2000.

In this study, we conducted similar aging experiments and examined the aged (brown) limonene secondary OA sample using nano-DESI. Figure 4 compares a selected m/z range from spectra of the brown limonene secondary OA sample obtained using ESI, DESI, and nano-DESI. AcN/water 1:1 (v/v) was used as the spray solvent for ESI and nano-DESI experiments, while the DESI spectrum adopted from our previous study[44] required 0.05% (vol) of trifluoroacetic acid (TFA) in the 1:1 (v/v) mixture of AcN and water. We note that only a very weak DESI signal was obtained without the addition of a strong acid. All three spectra contain abundant peaks corresponding to the original constituents of fresh (white) limonene secondary OA, composed of C, H, and O atoms only and cationized by Na^+. These species have odd nominal masses and form a long series of homologous peaks separated by masses of CH_2 and O, described in previous publications.[26,34] Peaks that are unique to aged (brown) limonene secondary OA appear at even masses and correspond to protonated N-containing species.[44]

Similar mass spectra were obtained using DESI and nano-DESI showing the presence of abundant oligomeric O- and N-containing species. Most N-containing species are observed at even nominal mass. In contrast, the majority of peaks in the ESI-MS spectrum of limonene secondary OA samples are observed at odd nominal masses. Clearly, even-m/z peaks are strongly suppressed or absent in the ESI-MS spectrum, while both DESI and nano-DESI spectra contain a large number of these species. In addition, the larger oligomers are observed with greater intensity by both nano-DESI and DESI than they are by ESI. For example, the series of characteristic polymeric manifolds of limonene secondary OA (data not shown) observed through the pentamer in both nano-DESI and DESI were observed only through the trimer for ESI.[27] These differences have been previously attributed to the decomposition of chemically labile oligomeric species during either the extraction process or the subsequent residence time in the solvent.[44] This suggests that the solvent residence time of OA in a nano-DESI experiment is sufficiently short to preserve these labile chemical bonds.

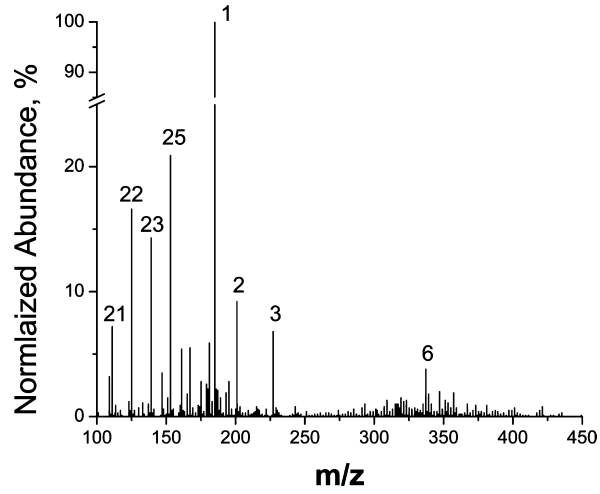

Figure 5. Nano-DESI/HR-MS spectrum of biomass burning OA sample. Abundant peaks observed in the spectrum are listed in Table. 1.

Although very similar mass spectra were obtained for limonene secondary OA samples using DESI and nano-DESI, we note that nano-DESI presents several advantages for mass spectrometric characterization of OA. For example, whereas DESI-MS analysis required the addition of the strong acid, TFA, no acid was required for nano-DESI analysis. Peaks in the pentamer region were observed with greater relative intensity by nano-DESI than by DESI. We attribute this difference to the greater stability and intensity of the signal that was achieved by nano-DESI in comparison with DESI, rather than to any physical differences in the sampling of the analyte or the respective extraction processes. Additionally, whereas the DESI source required the continuous XY translation of the sample to maintain a stable ion current, the nano-DESI source required only minimal adjustments per dozen minutes.

Figure 5 shows a nano-DESI/HR-MS spectrum of the biomass burning OA sample obtained from burning of ponderosa pine needles and sticks (PPNS) in the FLAME experiment. In this experiment 1:1 (v/v) MeOH/water was used as a spray solvent to facilitate comparisons with our previous ESI-MS analysis of the same sample.[31,32] Approximately 700 distinct species were identified in the nano-DESI spectrum. The majority of the identified peaks correspond to sodiated ions of oxygenated hydrocarbons ($C_xH_yO_zNa^+$), protonated N-containing oxygenated hydrocarbons ($C_xH_yO_zN_{1-2}H^+$), and N-containing heterocyclic compounds without oxygen detected as protonated species ($C_xH_yN_2H^+$). The most abundant peaks are listed in Table 1. The species that were not observed by the previous ESI analysis are highlighted in bold. There is very close agreement between the species identified by ESI and nano-DESI analyses, with more peaks detected by nano-DESI. However, the relative abundance of N-containing heterocyclic compounds is significantly enhanced in the nano-DESI spectrum with respect to the ESI-MS spectrum that was dominated by O-containing compounds.[31] The enhanced sensitivity toward N-containing heterocyclic compounds could be attributed to differences in extraction efficiencies in ESI-MS and nano-DESI experiments, to differences in the pH of the analyte solutions produced by online nano-DESI extraction and by ultrasonic rinsing used in ESI-MS experiments, or to an increased

Table 1. Abundant Peaks Observed in the Nano-DESI Spectrum of the Biomass Burning OA Sample Shown in Figure 5[a]

$C_xH_yO_z$ species				$C_xH_yO_zN$ species				$C_xH_yN_2$ species			
no.	*m/z*	abundance (%)	formula	no.	*m/z*	abundance (%)	formula	no.	*m/z*	abundance (%)	formula
1	185.042	100	$C_6H_{10}O_5Na^+$	11	124.076	0.5	$C_7H_9ONH^+$	21	111.092	7.2	$C_6H_{10}N_2H^+$
2	201.016	9.2	$C_9H_6O_4Na^+$	12	130.159	0.7	$C_8H_{19}NH^+$	22	125.107	16.6	$C_7H_{12}N_2H^+$
3	227.052	6.8	$C_8H_{12}O_6Na^+$	13	160.075	0.9	$C_{10}H_9ONH^+$	23	139.123	14.3	$C_8H_{14}N_2H^+$
4	**319.225**	**1.5**	$\mathbf{C_{18}H_{32}O_3Na^+}$	14	174.092	0.7	$C_{11}H_{11}ONH^+$	24	147.092	3.5	$C_9H_{10}N_2H^+$
5	337.177	1.6	$C_{20}H_{26}O_3Na^+$	15	**180.087**	**2.2**	$\mathbf{C_6H_{13}O_5NH^+}$	25	153.139	20.9	$C_9H_{16}N_2H^+$
6	337.235	3.8	$C_{18}H_{34}O_4Na^+$	16	188.107	0.5	$C_{12}H_{13}ONH^+$	26	161.107	5.4	$C_{10}H_{12}N_2H^+$
7	339.193	1.8	$C_{20}H_{28}O_3Na^+$	17	200.107	0.6	$C_{13}H_{13}ONH^+$	27	167.154	5.5	$C_{10}H_{18}N_2H^+$
8	347.094	2	$C_{12}H_{20}O_{10}Na^+$	18	216.102	0.6	$C_{13}H_{13}O_2NH^+$	28	175.123	2.8	$C_{11}H_{14}N_2H^+$
9	**351.192**	**1.3**	$\mathbf{C_{21}H_{28}O_3Na^+}$	19	230.117	0.5	$C_{14}H_{15}O_2NH^+$	29	181.170	5.9	$C_{11}H_{20}N_2H^+$
10	357.203	1.9	$C_{20}H_{30}O_4Na^+$	20	**318.242**	**0.7**	$\mathbf{C_{20}H_{31}O_2NH^+}$	30	195.186	2.8	$C_{12}H_{22}N_2H^+$

[a] Species that were not observed in the ESI spectrum of this sample[31,32] are marked in bold.

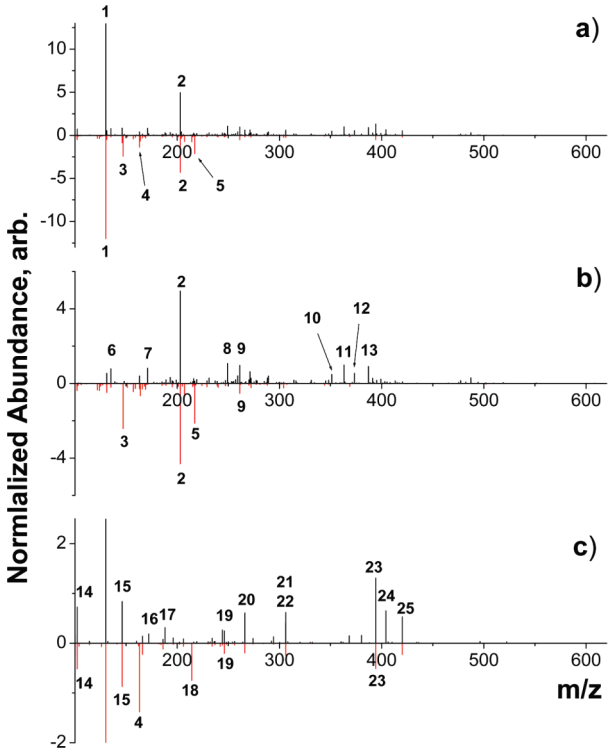

Figure 6. Nano-DESI/HR-MS spectra of Mexico City OA samples showing (a) all peaks, (b) peaks containing oxygen but no nitrogen, (c) all nitrogen-containing peaks. The results are plotted as negative (red) and positive (black) signal for samples collected during early morning (6 a.m.−9 a.m.) and noon (11 a.m.−2 p.m.) time periods, respectively. Abundant peaks labeled in the spectra are listed in Table 2.

concentration of sodium ions from the glassware used in ESI-MS extraction experiments. Because nano-DESI utilizes a small amount of solvent, it is reasonable to assume that the pH of the resulting solution is lower than was present in ESI-MS experiments, which in turn facilitates ionization of the more basic N-containing molecules as protonated species in nano-DESI.

The nano-DESI/HR-MS spectra obtained from the Mexico City OA ambient samples are shown in Figure 6. The samples were analyzed using a 1:1 (v/v) AcN/water spray solution. Unique chemical formulas were identified for approximately 200 individual species in each of the two samples collected at the early morning (6 a.m.−9 a.m.) and mid-day (11 a.m.−2 p.m.) time periods. The abundant peaks observed in the nano-DESI spectra of the Mexico City OA samples are listed in Table 2. Aiken et al.[54] have identified four major components of the Mexico City OA from real-time measurements using an aerosol mass spectrometer (AMS) that were conducted at the same sampling site. The identified components include oxygenated OA, most likely a surrogate for secondary OA, hydrocarbon-like OA related to vehicle emissions, biomass burning OA, and a "local" OA characterized by elevated concentrations of nitrogen-containing compounds which were attributed to amines from local industrial emissions.[55] Relative contributions of these four components to total Mexico City OA have a distinct diurnal profile[54] driven by day/night meteorological effects, changes in intensity of traffic emissions, and day-time photochemistry. As a result, hydrocarbon-like OA dominate during the night and early morning hours, while oxygenated OA becomes a major contributor during the day time. Relative contributions of biomass burning OA and "local" OA components do not change significantly during the day. The total OA mass measured by AMS at the time of the sampling was in the range of 10−20 $\mu g/m^3$, which would correspond to a mass of 55−110 μg being sampled on all stages of MOUDI from 5.4 m^3 of ambient air (3 h of sampling at 30 slpm flow rate). Using the very conservative assumption that all this mass was deposited on a single impaction stage, we estimate that less than 10 ng of analyte was required to generate high-quality spectra of Mexico City OA samples using nano-DESI/HR-MS.

An examination of the mass spectra obtained from the Mexico City OA samples reveals qualitative agreement with the AMS data reported by Aiken et al.[54] Several abundant peaks with relatively low molecular weight (m/z = 100−250) are common for both samples. The corresponding organic species are likely related to local emission sources. For instance, the most abundant $C_6H_{12}O_6Na^+$ peak corresponds to sodiated sugar molecules that are common constituents of both primary OA and secondary

(54) Aiken, A. C.; Salcedo, D.; Cubison, M. J.; Huffman, J. A.; DeCarlo, P. F.; Ulbrich, I. M.; Docherty, K. S.; Sueper, D.; Kimmel, J. R.; Worsnop, D. R.; Trimborn, A.; Northway, M.; Stone, E. A.; Schauer, J. J.; Volkamer, R. M.; Fortner, E.; de Foy, B.; Wang, J.; Laskin, A.; Shutthanandan, V.; Zheng, J.; Zhang, R.; Gaffney, J.; Marley, N. A.; Paredes-Miranda, G.; Arnott, W. P.; Molina, L. T.; Sosa, G.; Jimenez, J. L. *Atmos. Chem. Phys.* **2009**, *9*, 6633–6653.

(55) Moffet, R. C.; de Foy, B.; Molina, L. T.; Molina, M. J.; Prather, K. A. *Atmos. Chem. Phys.* **2008**, *8*, 4499–4516.

Table 2. Abundant Peaks Observed in Nano-DESI Mass Spectra of Mexico City OA Samples[a]

no.	*m/z*	formula	no.	*m/z*	formula	no.	*m/z*	formula
1	130.1589	$C_8H_{15}NH^+$	10	351.2009	$C_{16}H_{30}O_8H^+$	19	246.1699	$C_{12}H_{23}NO_4H^+$
2	203.0525	$C_6H_{12}O_6Na^+$	11	363.2373	$C_{18}H_{34}O_7H^+$	20	266.1961	$C_{12}H_{27}NO_5H^+$
3	147.1014	$C_7H_{14}O_3H^+$	12	373.2579	$C_{20}H_{36}O_6H^+$	21	306.1912	$C_{14}H_{27}NO_6H^+$
4	**163.1228**	$\mathbf{C_{10}H_{14}N_2H^+}$	13	387.0866	$C_{23}H_{14}O_6H^+$	22	306.2274	$C_{15}H_{31}NO_5H^+$
5	217.1798	$C_{12}H_{24}O_3H^+$	**14**	**102.1277**	$\mathbf{C_6H_{15}NH^+}$	23	394.2215	$C_{21}H_{31}NO_6H^+$
6	135.1014	$C_6H_{14}O_3H^+$	15	146.1174	$C_7H_{15}NO_2H^+$	24	404.2059	$C_{22}H_{29}NO_6H^+$
7	171.1016	$C_9H_{14}O_3H^+$	16	172.1333	$C_9H_{17}NO_2H^+$	25	420.2009	$C_{22}H_{29}NO_7H^+$
8	249.1696	$C_{12}H_{24}O_5H^+$	17	188.1283	$C_9H_{17}NO_3H^+$			
9	261.1697	$C_{13}H_{24}O_5H^+$	18	214.2529	$C_{14}H_{31}NH^+$			

[a] Numbered peaks correspond to labels in Figure 6. Species in OA from an urban environment of Shanghai reported by Wang et al.[16] are marked in bold.

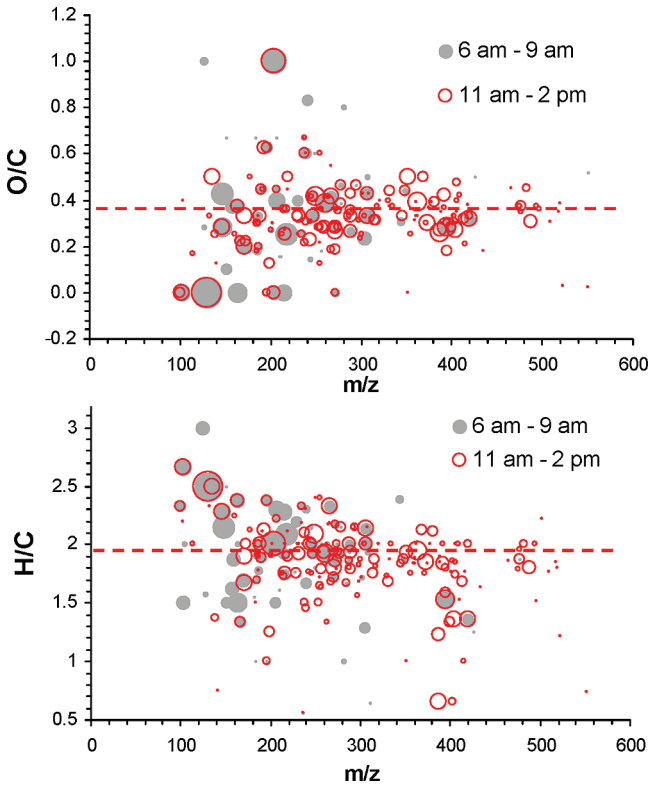

Figure 7. Atomic ratios of O/C and H/C in individual neutral species identified in Mexico City OA samples by nano-DESI/HR-MS analysis. The size of the points is proportional to the logarithm of the peak intensity. Dashed red lines indicate mean values of O/C and H/C ratios of species present in the day sample.

OA.[56] Other abundant species correspond to N-containing ions ($C_8H_{15}NH^+$; $C_{10}H_{14}N_2H^+$) that can be attributed to amines associated with the "local" OA component reported by the AMS data. The most notable difference between the morning and afternoon spectra is appearance of additional peaks in the higher M_w mass range ($m/z = 250-500$) that can be attributed to the presence of oligomer products in the afternoon sample that are absent in the morning. Processes leading to formation oligomers in OA have been extensively discussed in the literature based on laboratory measurements of secondary OA proxies.[20,22,26,27] However, field data establishing significance of these in ambient samples is still scarce. A recent study by Wang et al.[16] reported on formation of these products in the urban environment of Shanghai and attributed their reaction chemistry to aldol condensation and Manich reactions of aldehydes and ketones with amines. It is interesting to note that the oligomer species observed in the afternoon sample are mainly oxygenated organic compounds, which agrees with enhanced concentration of oxygenated OA derived from the AMS data.[54]

Figure 7 shows plots of O/C and H/C ratios corresponding to neutral individual species identified in two Mexico City OA samples and provide additional insights into the chemical composition of the Mexico City OA. Low molecular weight (M_w) species that originate from variety of local emission sources are present in both the morning and the noon samples and are characterized by a broad distribution of O/C and H/C ratios. In contrast, a much narrower distribution of O/C and H/C ratios is obtained for the higher M_w oligomeric species observed in the noon sample. Specifically, O/C and H/C ratios of higher M_w molecules are narrowly distributed around the mean values of 0.37 and 1.95, respectively. The mean ratios are notably close to the diurnal average values of O/C = 0.42−0.47 and H/C = 1.57−1.65 obtained for the time period of 11a.m.−2 p.m. from the AMS measurements over the entire duration of the MILAGRO field study.[57]

N-containing species comprise approximately 40% and 50% of the individual molecules identified in the morning and the noon Mexico City OA samples, respectively (see Figure S2 in the Supporting Information). A vast majority of N-containing organics, and notably oligomeric products, contain only one N atom (see Figure S3 in the Supporting Information). These observations are consistent with plausible particle-phase oligomerization chemistry which links amine/ammonia and aldehyde/carbonyl species through newly formed −C−N=C− chemical bonds.[16,44] Formation of these low-volatility products may play an important role in secondary OA formation in the urban environment, which is not well understood and severely underestimated by present models.[58]

(56) Simoneit, B. R. T.; Elias, V. O.; Kobayashi, M.; Kawamura, K.; Rushdi, A. I.; Medeiros, P. M.; Rogge, W. F.; Didyk, B. M. *Environ. Sci. Technol.* **2004**, *38*, 5939–5949.

(57) Aiken, A. C.; DeCarlo, P. F.; Kroll, J. H.; Worsnop, D. R.; Huffman, J. A.; Docherty, K. S.; Ulbrich, I. M.; Mohr, C.; Kimmel, J. R.; Sueper, D.; Sun, Y.; Zhang, Q.; Trimborn, A.; Northway, M.; Ziemann, P. J.; Canagaratna, M. R.; Onasch, T. B.; Alfarra, M. R.; Prevot, A. S. H.; Dommen, J.; Duplissy, J.; Metzger, A.; Baltensperger, U.; Jimenez, J. L. *Environ. Sci. Technol.* **2008**, *42*, 4478–4485.

(58) Hodzic, A.; Jimenez, J. L.; Madronich, S.; Aiken, A. C.; Bessagnet, B.; Curci, G.; Fast, J.; Lamarque, J. F.; Onasch, T. B.; Roux, G.; Schauer, J. J.; Stone, E. A.; Ulbrich, I. M. *Atmos. Chem. Phys.* **2009**, *9*, 6949–6981.

CONCLUSIONS

Detailed chemical characterization of OA is crucial for understanding the effect of different classes of organic compounds that are present in atmospheric particulate matter on the climate-related physical and chemical properties of aerosols. In this study, we presented the first application of a novel nano-DESI ionization technique combined with HR-MS for the analysis of both laboratory generated and field collected OA. The nano-DESI technique possesses distinct advantages over ESI and DESI ionization methods with respect to simplicity, ease of use, sensitivity, and signal stability. Similarly to DESI, nano-DESI eliminates the requirement for special sample preparation. OA collected on common substrates that are widely utilized in aerosol science such as Teflon or aluminum are readily analyzed using this approach, which provides high-quality HR-MS spectra using fairly small amounts of material (<10 ng). Stable signals obtained using nano-DESI are advantageous for conducting MS/MS experiments for structural characterization of OA constituents.

We demonstrate the utility of nano-DESI for the analysis and studies of chemical aging of laboratory generated secondary OA. Similarly to DESI, nano-DESI is shown to be capable of detecting chemically labile compounds responsible for the "browning" of secondary OA. Previous studies demonstrated that the conjugated N-containing compounds produced through condensation reactions in the chemical aging process and responsible for the absorption of the visible light by the brown limonene secondary OA are difficult to detect using traditional solvent extraction combined with ESI-MS analysis because of acid-catalyzed decomposition of these labile molecules. In contrast, both DESI and nano-DESI provide important information on the structure of chemically labile N-containing products of the chemical aging of secondary OA.

The high sensitivity and stability of nano-DESI enables characterization of small amounts of field-collected OA samples. Nano-DESI analysis of biomass burning OA samples provided high-quality HR-MS data that are in good qualitative agreement with the results reported in our previous ESI-MS study. Finally, the new technique has been applied for the analysis of samples collected during MILAGRO studies. The results of this analysis indicate the formation of oligomeric organic species through photochemical and chemical aging of primary OA and the presence of a significant amount of N-containing molecules in Mexico City OA samples.

ACKNOWLEDGMENT

The research was supported by the intramural research and development program of the W. R. Wiley Environmental Molecular Sciences Laboratory (EMSL), a national scientific user facility sponsored by the U.S. Department of Energy's Office of Biological and Environmental Research. EMSL is located at the Pacific Northwest National Laboratory (PNNL) operated by Battelle for the U.S. DOE. Patrick Roach acknowledges the support from the Chemical Sciences Division, Office of Basic Energy Sciences of the U.S. DOE.

SUPPORTING INFORMATION AVAILABLE

Additional information as noted in text. This material is available free of charge via the Internet at http://pubs.acs.org.

Received for review June 2, 2010. Accepted July 8, 2010.

AC101449P